

# Photoinduced Size Change of Membrane Vesicles from Bovine Retinal Rod Outer Segment†

William F. Hoffman,‡ Takashi Norisuye,§ and Hyuk Yu\*

**ABSTRACT:** Quasielastic light-scattering measurements were made on isolated, osmotically swollen, bovine rod outer segment (ROS) disk membranes in aqueous Ficoll. The translational diffusion coefficients determined were  $(1.66 \pm 0.21) \times 10^{-9}$  and  $(2.31 \pm 0.14) \times 10^{-9}$  cm<sup>2</sup>/s at 25 °C for the unbleached and bleached membranes in 5% Ficoll, respectively,

yielding the Stokes radii of  $0.53 \pm 0.07$   $\mu$ m for the former and  $0.38 \pm 0.02$   $\mu$ m for the latter. This photoinduced size decrease, which corresponds to a 60% decrease in the intravesicular volume, is far more pronounced than those reported by others for ROS fragments.

Photoreceptor rod outer segment (ROS)<sup>1</sup> fragments (disks + plasma membrane) swell and contract in response to change in the osmotic pressure of the bathing medium. Heller et al. (1970) and subsequently McConnell (1975) observed that the volume of ROS fragments was slightly decreased upon exposure to light. This photoinduced volume change may reflect a change in the permeability of the disks to certain ions or a transmitter substance whose subsequent interactions with receptors on the rod plasma membrane initiate the visual impulse (Hagins, 1972). Heller et al. attributed the observed permeability change of the ROS fragments to a change in that of the disks alone. It is quite possible, however, that the permeability of the plasma membrane also changes, as suggested by McConnell (1975). Thus, it is unclear whether the photoinduced volume changes of the ROS fragments result from permeability changes of the disks, the rod plasma membrane, or both. Any attempt to resolve this question requires study of the disks separate from the plasma membrane.

Very recently, we have found that isolated, osmotically swollen, bovine ROS disk membranes are extremely monodisperse vesicles whose radius as determined by elastic light scattering is the same as the Stokes radius (Norisuye et al., 1976). Therefore, quasielastic light scattering (QLS) with a 3-mW He/Ne laser light source (632.8-nm wavelength) makes it possible to determine the volume of unbleached and bleached membrane vesicles if their shapes can be approximated as spherical. The present study was undertaken to explore the size dependence of the vesicles on their photochemical state.

## Experimental Procedure

**Material.** Bovine ROS disk membranes were isolated and purified from frozen retinæ (Hormel Co.) by the method of Smith et al. (1975). The details were described previously (Norisuye et al., 1976). The ratio of the absorbance  $A_{278}$  at 278 nm to  $A_{498}$  at 498 nm was substantially constant ( $2.51 \pm 0.26$ ) for each independent preparation. The slight variation

in this ratio did not affect the QLS results for either unbleached or bleached membranes.

**Suspending Medium.** Preliminary QLS experiments showed that the ROS disk membranes had no tendency to aggregate in either aqueous Ficoll or aqueous sucrose. In this work, we used aqueous Ficoll (Type 400; Sigma) as the suspending medium for the QLS measurements, because Ficoll is known to be inert in many biological systems.<sup>2</sup> Ficoll is a highly branched, nonionic, water-soluble macromolecule having an average molecular weight of  $4 \times 10^5$  and a Stokes radius of 100 Å (Ficoll 400 is designated simply as Ficoll unless noted otherwise). Since the value of 100 Å for the Stokes radius is much smaller than that of our ROS vesicles (4000–5000 Å, see below), the spectral profile of scattered intensity of Ficoll is expected to be much broader than the frequency range of interest for the membranes. Furthermore, we have found that the scattered intensity of 8% Ficoll (the highest concentration used) is only 3% relative to that of our membrane solutions at any given angle. Therefore, we may safely ignore any contribution from Ficoll to the scattered intensity of the membrane suspensions.

**Quasielastic Light Scattering.** The instrument, the data acquisition scheme, and the spectrum analysis method have been described elsewhere (Shaya et al., 1974). The power spectrum  $S(\nu)$  of quasielastically scattered light was detected with use of the homodyne beat technique and analyzed by the equation of single Lorentzian type (Cummins and Swinney, 1970):

$$S(\nu) = A \frac{\Delta\nu_{1/2}}{\nu^2 + (\Delta\nu_{1/2})^2} + B \quad (1)$$

where  $A$  and  $B$  are constants representing the integrated spectral intensity and the apparent shot noise, respectively, and  $\nu$  is the frequency broadening from the incident frequency. The half-width at half-height of the single Lorentzian profile,  $\Delta\nu_{1/2}$ , is related to the translational diffusion coefficient  $D$  of a scattering particle by (Cummins and Swinney, 1970; Pecora, 1972; Chu, 1974)

$$\Delta\nu_{1/2} = D\kappa^2/\pi \quad (2)$$

where  $\kappa$  is the magnitude of scattering vector defined by  $(4\pi/\lambda') \sin(\theta/2)$  with the wavelength of light  $\lambda'$  in the scat-

† From the Department of Chemistry, University of Wisconsin, Madison, Wisconsin 53706. Received October 19, 1976. Supported by National Institutes of Health Grant EY01483.

‡ Wisconsin Alumni Research Foundation fellow and National Science Foundation predoctoral trainee.

§ On leave from the Department of Polymer Science, Osaka University, Toyonaka, Osaka, Japan.

† Abbreviations: ROS, rod outer segment; QLS, quasielastic light scattering.

<sup>2</sup> Separation News, Pharmacia Fine Chemicals, January 1973.

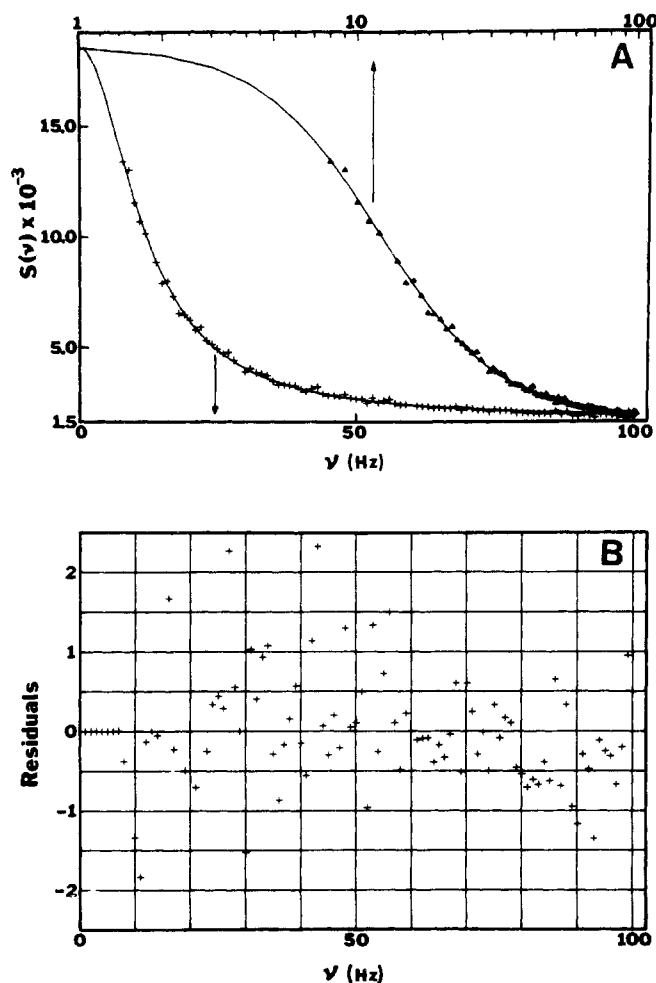


FIGURE 1: (A) Doppler broadened power spectrum of scattered light for the unbleached bovine ROS disk membranes in 5% aqueous Ficoll at an angle of 55 °C. Each solid curve (lower abscissa, linear frequency scale; upper abscissa, logarithmic frequency scale) is a single Lorentzian profile with the half-width at half-height,  $\Delta\nu_{1/2}$ , of 12.1 Hz, the integrated spectral intensity  $A$  of  $2.15 \times 10^5$ , and the apparent shot noise  $B$  of  $1.60 \times 10^3$ . (B) Normalized residuals plot of A. The ordinate is defined as  $[(n-1)]^{1/2}[S(\nu_i) - S_0(\nu_i)]/\{\sum_i [S(\nu_i) - S_0(\nu_i)]^2\}^{1/2}$ , where  $n$  is the number of data points (100) in the power spectrum, and  $S(\nu_i)$  and  $S_0(\nu_i)$  are respectively the experimental spectral intensity and the predicted intensity with the parameter set for the single Lorentzian profile in A both at frequency  $\nu_i$ .

tering medium and scattering angle  $\theta$ . Determinations of the three parameters,  $A$ ,  $\Delta\nu_{1/2}$ , and  $B$ , in eq 1 were effected via a nonlinear regression method on a Univac 1110 computer, and then  $D$  was evaluated from the slope of a plot of  $\Delta\nu_{1/2}$  against  $\kappa^2/\pi$  (see below for the details). The following sets of measurements were performed at room temperature ( $25.1 \pm 0.3$  °C): (1) the unbleached membrane suspensions at two different concentrations (5 and 6% by weight) of aqueous Ficoll and (2) the bleached membrane suspensions at four different concentrations in the range of 3–8% aqueous Ficoll. All data except the two data sets for the unbleached membranes in 5% Ficoll were taken with a polarizer and an analyzer both set in the vertical direction with respect to the scattering plane; for the two data sets, neither polarizer nor analyzer was inserted along the beam path. The incident light was a 3-mW He/Ne laser beam (632.8 nm; Spectra-Physics 135).

Membrane suspensions for QLS measurements were prepared in the same manner as described previously (Norisuye et al., 1976). Both the unbleached and bleached membrane suspensions were stable at 25 °C for about 5 h as judged by the

constancy of their translational diffusion coefficients  $D$ . However, after 5 h,  $D$  became appreciably larger, suggesting that the size of membranes became smaller. The size change, which is probably due to bursting of the membranes and re-sealing into smaller vesicles, has also been observed by Raubach et al. (1974). Therefore, all QLS measurements were completed within 5 h (in most cases, within 2.5 h) after purification.

Since the QLS measurement necessitates the exposure of the membranes to a red light (632.8 nm), we examined its effects on the photochemical state of the membranes. No detectable difference was observed between the absorbance ratios  $A_{278}/A_{498}$  before and after the QLS measurement on an unbleached membrane suspension. However, this cannot be taken as direct evidence for negligible effect of the exposure since the narrow laser beam (3 mm in diameter) shines upon only a small fraction of the whole suspension. Therefore, a more informative test was performed wherein the laser beam was made to illuminate most of the suspension in a long, narrow tube (3.6 mm inside diameter and 25 cm length) for a period comparable to QLS measurements, and the absorbances were subsequently examined. The results showed a roughly linear decrease in  $A_{498}$  of 10% per h over a period of 3 h. On the other hand, no time dependence of  $D$  in the unbleached state was found within a comparable period after the preparation. As described below, there exists a significant difference in the diffusion coefficients between the unbleached and bleached states, so that it seems unreasonable to ascribe the  $A_{498}$  decrease to bleaching (i.e., transformation of 11-*cis*-retinal to *all-trans*-retinal). Since rhodopsin is known to assume several photoisomeric states at intermediate stages in bleaching process (Yoshizawa and Wald, 1963), we attribute the observed decrease in  $A_{498}$  to the formation of such an isomer as bathorhodopsin (Busch et al., 1972; Oseroff and Callender, 1974) which is not attended by change in  $D$  of the membranes. As for the exact photochemical state that is induced by a red laser in our membrane suspensions, a further study is required.

## Results and Discussion

**Analysis of Spectral Data.** A Doppler broadened power spectrum of scattered light from the unbleached ROS disk membranes in 5% Ficoll at an angle of 55° is shown in Figure 1A, and the corresponding normalized residuals plot is given in Figure 1B, where deviations of the data points from the single Lorentzian with the half-width  $\Delta\nu_{1/2}$  of 12.1 Hz are plotted against linear frequency  $\nu$ . The random pattern of the residuals demonstrates that the data are well represented by the single Lorentzian profile, i.e., by eq 1. A similar result from the bleached membranes in 5% Ficoll at 70 °C is shown in Figure 2. Again, the single Lorentzian with  $\Delta\nu_{1/2}$  of 21.2 Hz is an excellent representation of the data. The angular dependence of  $\Delta\nu_{1/2}$  for the unbleached membrane suspensions in two different concentrations of Ficoll is displayed in Figure 3, where  $\Delta\nu_{1/2}$  is plotted against  $\kappa^2/\pi$  in accordance with eq 2. Independently prepared samples and the mode of polarization are distinguished by different symbols. It can be seen that the two sets of data points for different Ficoll concentrations follow respective straight lines which have a small but common intercept ( $3.5 \pm 0.2$  Hz) within the experimental error. The corresponding plot for the bleached membranes is shown in Figure 4. The four sets of data for different concentrations of Ficoll provide respective straight lines with a common intercept of  $3.4 \pm 0.2$  Hz which is the same as in the case of the unbleached membranes within the error limits. These finite positive intercepts are not in accord with the prediction

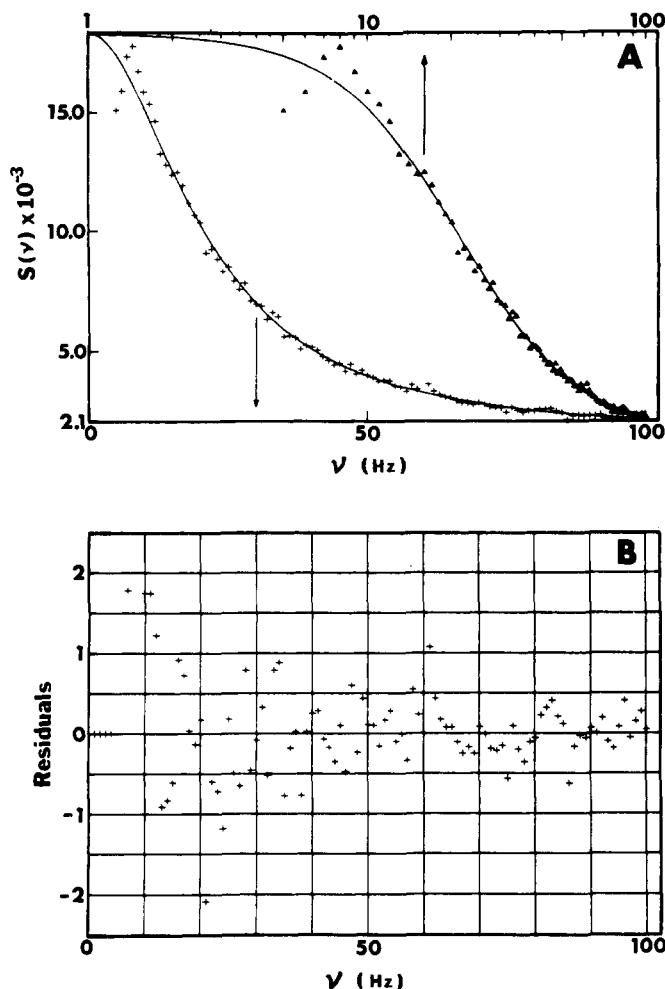


FIGURE 2: (A) Doppler broadened power spectrum of scattered light for the bleached membranes in 5% Ficoll at 70 °. Each solid curve represents a single Lorentzian profile with  $\Delta\nu_{1/2} = 21.2$  Hz,  $A = 7.89 \times 10^5$ , and  $B = 2.02 \times 10^3$ . (B) Normalized residuals plot of A.

of eq 2, although they are small. One could argue that the slopes no longer represent the translational diffusion coefficients  $D$ . As shown in the Appendix, however, the slopes can still be equated to  $D$ . Furthermore, from an elastic light scattering measurement performed for the bleached membranes in 0.88% aqueous Ficoll 70 (type 70; mol wt,  $7 \times 10^4$ ; Sigma), we have found that the membranes in this medium are spherical vesicles (see Appendix). Since its molar concentration is equivalent to 5% Ficoll 400 (most extensively used in this work), it is quite reasonable to assume that the membranes are spherical in aqueous Ficoll 400 as well. Once the spherical shape is accepted for our membranes in both photochemical states, we can evaluate the Stokes radii with use of  $D$  determined from the slopes of the straight lines in Figures 3 and 4.

**Size Determinations.** We calculate the Stokes radii  $R$  from the translational diffusion coefficients with use of the Stokes-Einstein equation

$$D = \frac{kT}{6\pi\eta_0 R} \quad (3)$$

where  $k$  is Boltzmann constant,  $T$  the absolute temperature, and  $\eta_0$  the viscosity of the suspending medium which was measured separately for each suspension with a capillary viscometer (Cannon-Ubbelohde type). All the numerical results for  $D$ ,  $\eta_0$ , and  $R$  are collected in Table I. The indicated

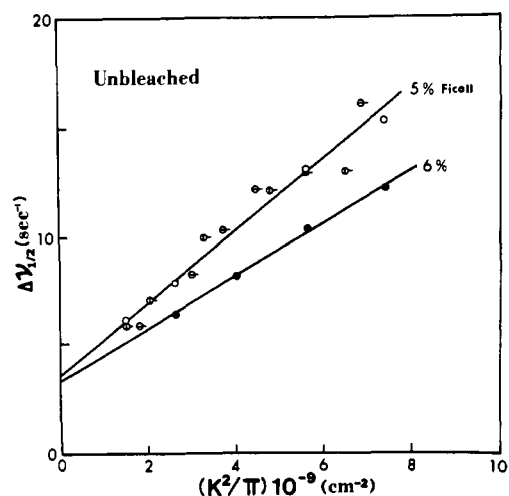


FIGURE 3: Plots of  $\Delta\nu_{1/2}$  vs.  $\kappa^2/\pi$  for the unbleached membranes in aqueous Ficoll of the two different concentrations. Independently prepared samples and modes of polarization are distinguished by different symbols: horizontal pip (unpolarized light) and no pip (vertical-vertical polarization configuration; see text). Each straight line is drawn according to least-squares analysis.

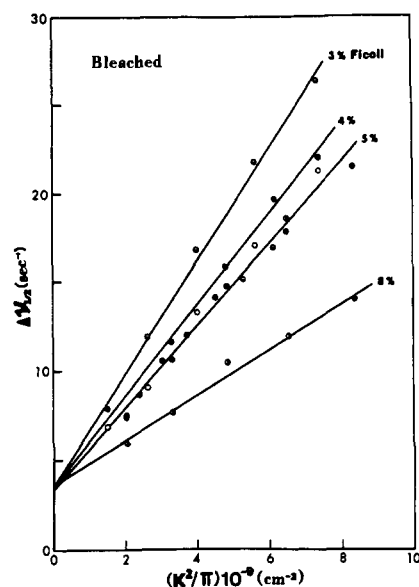


FIGURE 4: Plots of  $\Delta\nu_{1/2}$  vs.  $\kappa^2/\pi$  for the bleached membranes in aqueous Ficoll in the indicated concentrations.

uncertainties refer to the 95% confidence limits in the least-squares analysis with Student's  $t$  distribution for the errors in determining the slopes of the straight lines in Figures 3 and 4 (Draper and Smith, 1966). Since the membranes in 5% Ficoll are most extensively examined both for the unbleached and bleached states, the Stokes radii are most precisely determined as  $0.53 \pm 0.07$  and  $0.38 \pm 0.02$   $\mu\text{m}$ , respectively, by virtue of a large number of degrees of freedom for each set (Draper and Smith, 1966). These values would indicate that the Stokes radius of the unbleached membranes decreases by 28% upon bleaching. Upon taking into account the experimental uncertainties, the range of decrease in the radius is specified as 13–40%. As seen in Table I, the prediction of the Stokes-Einstein equation relative to the viscosity dependence is well borne out for both the unbleached and bleached states, which substantiates the reliability of our determination of  $D$ .

Two points are to be noted here: (1) Ficoll did not interfere with our power spectra because, if it had, we would not have

TABLE I: Translational Diffusion Coefficients  $D$  and Stokes Radii  $R$  for Unbleached and Bleached Bovine ROS Disk Membranes in Aqueous Ficoll and Aqueous Sucrose.

Suspending Medium <sup>a</sup>	Medium Viscosity (centipoise)	Unbleached <sup>b</sup>		Bleached <sup>b</sup>	
		$D \times 10^9$ (cm <sup>2</sup> /s) at 25 °C	$R$ (μm)	$D \times 10^9$ (cm <sup>2</sup> /s) at 25 °C	$R$ (μm)
3% Ficoll	1.67			3.15 ± 0.39	0.42 ± 0.05
4% Ficoll	2.05			2.57 ± 0.70	0.41 ± 0.12
5% Ficoll	2.46	1.66 ± 0.21	0.53 ± 0.07	2.31 ± 0.14	0.38 ± 0.02
6% Ficoll	3.09	1.21 ± 0.24	0.58 ± 0.12		
8% Ficoll	4.02			1.27 ± 0.31	0.43 ± 0.12
4.36 × 10 <sup>-3</sup> % sucrose	1.03			4.19 ± 0.45 <sup>c</sup>	0.51 ± 0.05 <sup>c</sup>

<sup>a</sup> Concentrations of Ficoll are approximate values except for 5% Ficoll. <sup>b</sup> All the indicated uncertainties refer to the 95% confidence limits (see text). <sup>c</sup> Taken from a previous paper (Norisuye et al., 1976).

obtained the Stokes radii independent of Ficoll concentration in respective photochemical states and (2) any osmotic pressure effect arising from the change in Ficoll concentration was small within the limited concentration range examined because the change in  $D$  values appeared to be accountable for by the viscosity change alone. The uncertainty of  $D$  arising from the expedient of the single Lorentzian model used in this work does not alter the conclusions; its maximum uncertainty ( $\pm 10\%$ ; see Appendix) is always within the errors in determining the slopes of the straight lines in Figures 3 and 4 excepting the data for the bleached membranes in 5% Ficoll. In view of the previous finding (Norisuye et al., 1976), the Stokes radii are assumed to be the equilibrium radii of the membrane vesicles. It must be noted, however, that our previous finding is restricted to the bleached membranes in a dilute sucrose solution ( $\sim 4 \times 10^{-3}\%$  by weight) and hence equating of the Stokes radius with the equilibrium vesicular radius remains to be an assumption regardless of its reasonableness until confirmed explicitly. We might also add that the observed half-width had no detectable dependence on membrane concentration; this was expected inasmuch as our suspensions were dilute enough that the viscosity difference between a Ficoll solution and the corresponding membrane suspension did not amount to more than 6%. The maximum volume fraction of vesicles in our suspensions could not be more than 2.4% according to the Einstein equation for the viscosity of spherical suspensions.

We have also determined the translational diffusion coefficient and the Stokes radius for the unbleached membranes in  $4.36 \times 10^{-3}\%$  aqueous sucrose whose molar concentration is equivalent to 5% Ficoll. In contrast to the behavior in aqueous Ficoll, there was no size difference between the unbleached and bleached vesicles in this aqueous sucrose, so that in Table I we have recorded only the result for the bleached state (Norisuye et al., 1976). Effects of bathing medium on vesicular size are little known. It is of interest to note that the radius either for the unbleached or bleached vesicles in the sucrose solution is substantially the same as that for the unbleached vesicles in aqueous Ficoll. Exact nature of the difference between the two media is obscure and its elucidation must await further investigation.

**Photoinduced Size Change.** It has been demonstrated that a roughly 30% (13–40%) decrease in the radius of the membrane vesicles in aqueous Ficoll takes place upon bleaching. This corresponds to a decrease of the intravesicular volume by 60% (33–78%)—a change that is, even by taking the lower bound, much greater than the photoinduced volume changes reported by previous workers (Heller et al., 1970; McConnell,

1975) with vertebrate ROS fragments. For instance, Heller et al. (1970) observed 12–15% decrease. Although the photoinduced intravesicular volume decrease in vivo may not be as large as 60% as in our vesicles, an indication of such a contraction had been put forth by Worthington (1973) with frog ROS (*Rana pipiens*). Alternatively, one can recast the volume change into the change in surface area of the vesicles by 50%, which seems to indicate a broad range of the elastic modulus of these membranes and of the surface packing density of the intramembranous components. The photoinduced increase in the surface packing density by 50% (24–64%) is in qualitative accord with the x-ray diffraction result of Blasie (1972) with the disk membranes from frog *Rana pipiens* ROS.

Our findings may be explained on the basis of Hagins' model (1972) of the photoinduced  $\text{Ca}^{2+}$  gating as the primary excitation mechanism in the vertebrate retinal rod. There has accumulated a substantial body of evidence that the ROS disks release  $\text{Ca}^{2+}$  upon bleaching (Poo and Cone, 1973; Hagins and Yoshikami, 1974; Hendriks et al., 1974; Mason et al., 1974; Weller et al., 1975). It seems reasonable to expect then that the  $\text{Ca}^{2+}$  efflux from the intravesicular space will be photoinduced and that the subsequent increase in the chemical potential of water within the vesicle will promote the efflux of water toward the extravesicular space, resulting in a decrease of vesicular size. Furthermore, the increase of  $\text{Ca}^{2+}$  concentration in the extravesicular space near a vesicle may allow electrostatic interactions among the membrane surface components to be screened, also resulting in decrease of vesicular size. The former mechanism refers to the osmotic pressure change of the bathing medium due to the increase in concentration of free  $\text{Ca}^{2+}$  while the latter refers to the screening effect of electrostatic interactions probably due to the increase in number of  $\text{Ca}^{2+}$ 's bound to the extravesicular side of the membrane surface. If either mechanism is indeed responsible for the observed size decrease, then the size contraction should be attended by an increase in either free  $\text{Ca}^{2+}$  concentration in the extravesicular space or  $\text{Ca}^{2+}$  bound to the extravesicular membrane surface. An active investigation to correlate the change in vesicular size with the change in  $\text{Ca}^{2+}$  concentration is in progress in this laboratory.

Finally, we briefly discuss the small intercepts found in the linear plots of  $\Delta\nu_{1/2}$  vs.  $\kappa^2/\pi$  in Figures 3 and 4. We have confirmed that the intercepts are only due to these membrane suspensions and not due to any instrumental artifact such as the insufficient damping of vibrations of the optical mounts (see Appendix). If the membranes are indeed spherical in equilibrium shape, these intercepts cannot be attributed to the

contribution from rotatory diffusion but may be due to a contribution from other scattering angle independent modes such as surface motions of the vesicles. The present homodyne method is not appropriate for exploring internal modes of the vesicles as described in the Appendix. Instead, we could probe with the forward depolarized QLS technique by which only  $\kappa$ -independent terms are detected (Wada et al., 1969; Schurr and Schmitz, 1973; Han and Yu, 1974). This kind of study is inviting if there is a change in the surface vibrational dynamics accompanied by the change in packing density of the intramembranous components upon bleaching.

## Conclusions

In this work, we have, using the quasielastic light scattering technique, determined the translational diffusion coefficients  $D$  of osmotically swollen ROS disk membranes in 5% aqueous Ficoll as  $(1.66 \pm 0.21) \times 10^{-9} \text{ cm}^2/\text{s}$  for the unbleached state and  $(2.31 \pm 0.14) \times 10^{-9} \text{ cm}^2/\text{s}$  for the bleached state both at 25 °C. Upon assuming the spherical shape for the membrane vesicles in both photochemical states, the Stokes radii were calculated from  $D$  as  $0.53 \pm 0.07$  and  $0.38 \pm 0.02 \mu\text{m}$  for the unbleached and bleached states, respectively, amounting to a roughly 30% decrease in the vesicular radius upon bleaching. This photoinduced contraction can be explained qualitatively by Hagins' model (1972).

## Appendix

The purposes of this Appendix are (1) to show that the slope of each straight line in Figures 3 and 4 (hereafter referred as  $D_{\text{app}}$ ) is the same as the translational diffusion coefficient  $D$  within the uncertainty in determining the slope and (2) to elucidate the possible origin of the positive finite intercept of the plots in Figures 3 and 4. For the first, we carried out the elastic light scattering and QLS measurements for the bleached membranes in aqueous solution (0.88% by weight) of lower molecular weight Ficoll 70 (mol wt,  $7 \times 10^4$ ; Stokes radius, 51 Å; Sigma); note that Ficoll 400 was found to be unsuited for the elastic light scattering measurement because of its high molecular weight resulting in large background scatterings. The elastic light scattering data analyzed by the same procedure as described (Norisuye et al., 1976) were consistent with the spherical shell model for the membranes, giving the value of  $0.48 \pm 0.02 \mu\text{m}$  for the equilibrium radius. On the other hand, the plot of  $\Delta\nu_{1/2}$  vs.  $\kappa^2/\pi$  obtained from the QLS spectra in the same medium with the single Lorentzian model again gave a straight line whose slope and intercept were  $(4.90 \pm 0.24) \times 10^{-9} \text{ cm}^2/\text{s}$  and  $2.6 \pm 0.8 \text{ Hz}$ , respectively. If  $D_{\text{app}}$  is assumed to be equal to  $D$ , then the corresponding Stokes radius is deduced as  $0.44 \pm 0.04 \mu\text{m}$ , which is in fair agreement with the equilibrium radius  $0.48 \pm 0.02 \mu\text{m}$ . Since the Stokes radius of the bleached membranes in a dilute sucrose solution is shown to be the same as the equilibrium radius (Norisuye et al., 1976), this agreement indicates that  $D_{\text{app}}$  is the same as  $D$  within  $\pm 8\%$ , which hardly exceeds the uncertainties in the determinations of  $D_{\text{app}}$  (see Table I).

Having thus shown that the apparent diffusion coefficient can reasonably be equated to the true translational diffusion coefficient, we proceed with the discussion of the possible origin of the observed intercepts in the plots of  $\Delta\nu_{1/2}$  vs.  $\kappa^2/\pi$ . We are certain that the intercepts are not due to some spurious experimental artifact because they appear consistently with these vesicles but not with optically isotropic scatterers such as polystyrene latex. We therefore suspect that the observed power spectra might contain some additional components

beside the principal Lorentzian; however, their contributions were so small as to mask the attendant deviations from the single Lorentzian profile. The observed intercepts on the other hand might be due to these additional components. The argument in support of this contention is provided as follows.

We first note that the translational diffusion should be representable by a single Lorentzian profile since our membranes are homogeneous in size (see introductory section). Next, we postulate that the subsidiary components are also Lorentzian in profile which are attributed to the internal modes of the vesicles and hence independent of the scattering angle. Retaining only the largest contribution of such components, we may express the homodyne beat power spectrum  $S(\nu)$  (Berne and Pecora, 1976) as

$$S(\nu) = [P_0(\kappa)]^2 \frac{D\kappa^2/\pi}{\nu^2 + (D\kappa^2/\pi)^2} + [P_1(\kappa)]^2 \frac{(2C_1)}{\nu^2 + (2C_1)^2} + 2P_0(\kappa)P_1(\kappa) \frac{(D\kappa^2/2\pi) + C_1}{\nu^2 + [(D\kappa^2/2\pi) + C_1]^2} + B \quad (\text{A-1})$$

where the intensity factors  $P_0(\kappa)$  and  $P_1(\kappa)$  correspond to the translational diffusion and the predominant internal mode with the half-width  $2C_1$ , respectively. We then examine whether the power spectrum  $S(\nu)$  might still be representable as a single Lorentzian profile whose half-width is given by

$$\Delta\nu_{1/2} = D_{\text{app}}(\kappa^2/\pi) + C \quad (\text{A-2})$$

as all our experimental data, shown in Figures 3 and 4, are similarly expressed. We have simulated a series of spectra according to eq A-1 and analyzed them by the identical scheme as adopted for the experimental data. The following sets of the parameters were chosen:  $D = 2.5 \times 10^{-9} \text{ cm}^2/\text{s}$ ,  $3 \text{ Hz} \leq C_1 \leq 20 \text{ Hz}$  (both are comparable to  $D_{\text{app}}$  and  $C$ ; see Table I and Figures 3 and 4), and various values of  $P_1(\kappa)/P_0(\kappa)$  smaller than  $(\kappa R)^2$ . Here  $P_0(\kappa)$  was always assumed to be proportional to  $(\kappa R)^{-2}$  on the basis of the observed angular dependence of the total scattered intensity from a bleached membrane suspension in 5% Ficoll, whereas  $P_1(\kappa)$  was assumed to be independent of  $\kappa R$ . The single Lorentzian representation was judged by the criteria of randomness of the normalized residuals (see Figures 1 and 2) and small root-mean-square deviations. The results can be summarized as below.

(1) The single Lorentzian representation is entirely satisfactory within the same band width (6–100 Hz) as in the actual data acquisition if  $P_1(\kappa)/P_0(\kappa)$  is less than  $0.2(\kappa R)^2$ ; in fact, the quality of the fit is better than or comparable to that of the actual data for the membranes.

(2) In the cases where the single Lorentzian representation is satisfactory, its half-width approximately follows eq A-2 over the angular range displayed in Figures 3 and 4.

(3) The deduced  $D_{\text{app}}$  agrees with the input value of  $D$  within 10% (in most cases within 5%) while the intercept  $C$  depends on the ratio  $P_1(\kappa)/P_0(\kappa)$  but never exceeds the input  $C_1$  value.

These findings demonstrate that our fitting routine cannot distinguish, within the prevailing precision of data acquisition, the spectral profiles expressed by eq A-1 from the single Lorentzian profiles if  $P_1(\kappa)/P_0(\kappa) \leq 0.2(\kappa R)^2$  and  $3 \text{ Hz} \leq C_1 \leq 20 \text{ Hz}$ , and that the finite positive intercept  $C$  can be taken as a qualitative measure of the scattering angle independent component such as  $C_1$  mode in eq A-1.

We conclude from the foregoing that the slope of the observed linear plot of  $\Delta\nu_{1/2}$  vs.  $\kappa^2/\pi$  corresponds to  $D$  within the experimental uncertainty. It must be added here that none of

the attempts to decompose our spectra into the two Lorentzian components by use of eq A-1 was successful.

## References

- Berne, B. J., and Pecora, R. (1976), *Dynamic Light Scattering*, New York, N.Y., Wiley.
- Blasie, J. K. (1972), *Biophys. J.* 12, 205.
- Busch, G. E., Applebury, M. L., Lamola, A. A., and Rentzepis, P. (1972), *Proc. Natl. Acad. Sci. U.S.A.* 69, 2802.
- Chu, B. (1974), *Laser Light Scattering*, New York, N.Y., Academic Press.
- Cummins, H. Z., and Swinney, H. L. (1970), in *Progress in Optics*, Vol. VIII, Walf, E., Ed., Amsterdam, North-Holland Publishing Co.
- Draper, N. R., and Smith, H. (1966), *Applied Regression Analysis*, New York, N.Y., Wiley.
- Hagins, W. A. (1972), *Annu. Rev. Biophys. Bioeng.* 1, 131.
- Hagins, W. A., and Yoshikami, S. (1974), *Exp. Eye Res.* 18, 299.
- Han, C. C.-C., and Yu, H. (1974), *J. Chem. Phys.* 61, 2650.
- Heller, J., Ostwald, T. J., and Bok, D. (1970), *Biochemistry* 9, 4884.
- Hendriks, Th., Daemen, F. J. M., and Bonting, S. L. (1974), *Biochim. Biophys. Acta* 345, 468.
- Mason, W. T., Fager, R. S., and Abrahamson, E. W. (1974), *Nature (London)* 247, 562.
- McConnell, D. G. (1975), *J. Biol. Chem.* 250, 1898.
- Norisuye, T., Hoffman, W. F., and Yu, H. (1976), *Biochemistry* 15, 5678.
- Oseroff, A. R., and Callender, R. H. (1974), *Biochemistry* 13, 4243.
- Pecora, R. (1972), *Annu. Rev. Biophys. Bioeng.* 1, 257.
- Poo, M. M., and Cone, R. A. (1973), *Exp. Eye Res.* 17, 503.
- Raubach, R. A., Nemes, P. P., and Dratz, E. A. (1974), *Exp. Eye Res.* 18, 1.
- Schurr, J. M., and Schmitz, K. S. (1973), *Biopolymers* 12, 1021.
- Shaya, S. A., Han, C. C.-C., and Yu, H. (1974), *Rev. Sci. Instrum.* 47, 280.
- Smith, Jr., H. G., Stubbs, G. W., and Litman, B. J. (1975), *Exp. Eye Res.* 20, 211.
- Wada, A., Suda, N., Tsuda, T., and Soda, K. (1969), *J. Chem. Phys.* 50, 31.
- Weller, M., Virmaux, N., and Mandel, P. (1975), *Nature (London)* 256, 68.
- Worthington, C. R. (1973), *Exp. Eye Res.* 17, 487.
- Yoshizawa, T., and Wald, G. (1963), *Nature (London)* 197, 1279.

# Stabilization by the 30S Ribosomal Subunit of the Interaction of 50S Subunits with Elongation Factor G and Guanine Nucleotide<sup>†</sup>

Robert C. Marsh<sup>‡</sup> and Andrea Parmeggiani<sup>\*§</sup>

**ABSTRACT:** The role of the 30S ribosomal subunit in the formation of the complex ribosome-guanine nucleotide-elongation factor G (EF-G) has been examined in a great variety of experimental conditions. Our results show that at a large molar excess of EF-G or high concentrations of GTP or GDP, 50S ribosomal subunits are as active alone as with 30S subunits in the formation of the complex, while at lower concentrations of nucleotide or lower amounts of EF-G, addition of the 30S subunit stimulates greatly the reaction. The presence of the 30S ribosomal subunit can also moderate the inhibition of the 50S subunit activity that occurs by increasing moderately the concentrations of K<sup>+</sup> and NH<sub>4</sub><sup>+</sup>, and extends upward the

concentration range of these monovalent cations in which complex formation is at maximum. The Mg<sup>2+</sup> requirement for complex formation with the 50S subunit appears to be slightly less than that needed for association of the 30S and 50S ribosomal subunits. Measurement of the reaction rate constants of the complex formation shows that the 30S ribosomal subunit has only little effect on the initial association of EF-G and guanine nucleotide with the 50S subunit; but once this complex is formed, the 30S subunit increases its stability from 10- to 18-fold. It is concluded that stabilization of the interaction between EF-G and ribosome is a major function of the 30S subunit in the ribosome-EF-G GTPase reaction.

During protein synthesis, the interaction of the ribosome with elongation factor G (EF-G)<sup>1</sup> and the accompanying hy-

drolisis of GTP result in the translocation of peptidyl-tRNA from the ribosomal acceptor to donor site and movement relative to the mRNA (for review, see Haselkorn and Rothman-Denes, 1973). At low concentration of the monovalent cations K<sup>+</sup> and NH<sub>4</sub><sup>+</sup>, the 50S ribosomal subunit is fully capable of supporting a high level of EF-G-dependent GTP hydrolysis; but at higher, more physiological concentrations, the 30S ribosomal subunit is required (Voigt et al., 1974; Parmeggiani et al., 1974; Arai and Kaziro, 1975). To gain insight into the manner in which the 30S ribosomal subunit is involved, we have examined its role in the formation of EF-G-guanine nucleotide-ribosome complex, which represents a stabilized intermediate of the GTPase reaction.

<sup>†</sup> From Abteilung Biochemie Gesellschaft für Molekularbiologische Forschung, 3301 Braunschweig-Stöckheim, German Federal Republic, and Laboratoire de Biochimie, Ecole Polytechnique, 91128 Palaiseau Cedex, France. Received July 28, 1976. This work was supported by Grant Pa 106 from the Deutsche Forschungsgemeinschaft.

<sup>‡</sup> Present address: Molecular Biology Program, The University of Texas at Dallas, Richardson, Texas 75080.

<sup>§</sup> Present address: Laboratoire de Biochimie, Ecole Polytechnique, 91128 Palaiseau Cedex, France.

<sup>1</sup> Abbreviations used: EF-G, elongation factor G; GMPPCP, 5'-guanylmethylenediphosphonate; PEI, polyethylenimine; DEAE, diethylaminoethyl; Tris, tris(hydroxymethyl)aminomethane.